APPLIED AND ENVIRONMENTAL MICROBIOLOGY, June 2006, p. 4370–4381 Vol. 72, No. 6
0099-2240/06/$08.00+0 doi:10.1128/AEM.02609-05

Energetic Consequences of Nitrite Stress in *Desulfovibrio vulgaris* Hildenborough, Inferred from Global Transcriptional Analysis†

Qiang He,[1,2,3] Katherine H. Huang,[1,4] Zhili He,[1,2,10] Eric J. Alm,[1,4] Matthew W. Fields,[1,5] Terry C. Hazen,[1,6] Adam P. Arkin,[1,4,7,8] Judy D. Wall,[1,9] and Jizhong Zhou[1,2,10]*

Virtual Institute for Microbial Stress and Survival, Berkeley, California 94720[1]‡; Environmental Sciences Division, Oak Ridge National Laboratory, Oak Ridge, Tennessee 37831[2]; Department of Civil and Environmental Engineering, Temple University, Philadelphia, Pennsylvania 19122[3]; Physical Biosciences Division, Lawrence Berkeley National Laboratory, Berkeley, California 94720[4]; Department of Microbiology, Miami University, Oxford, Ohio 45056[5]; Earth Sciences Division, Lawrence Berkeley National Laboratory, Berkeley, California 94720[6]; Department of Bioengineering, University of California, Berkeley, California 94720[7]; Howard Hughes Medical Institute, Chevy Chase, Maryland 20815[8]; Departments of Biochemistry and Molecular Microbiology and Immunology, University of Missouri—Columbia, Columbia, Missouri 65211[9]; and Institute for Environmental Genomics, Department of Botany and Microbiology, University of Oklahoma, Norman, Oklahoma 73019[10]

Received 4 November 2005/Accepted 18 March 2006

Many of the proteins that are candidates for bioenergetic pathways involved with sulfate respiration in Desulfovibrio spp. have been studied, but complete pathways and overall cell physiology remain to be resolved for many environmentally relevant conditions. In order to understand the metabolism of these microorganisms under adverse environmental conditions for improved bioremediation efforts, *Desulfovibrio vulgaris* Hildenborough was used as a model organism to study stress response to nitrite, an important intermediate in the nitrogen cycle. Previous physiological studies demonstrated that growth was inhibited by nitrite and that nitrite reduction was observed to be the primary mechanism of detoxification. Global transcriptional profiling with whole-genome microarrays revealed coordinated cascades of responses to nitrite in pathways of energy metabolism, nitrogen metabolism, oxidative stress response, and iron homeostasis. In agreement with previous observations, nitrite-stressed cells showed a decrease in the expression of genes encoding sulfate reduction functions in addition to respiratory oxidative phosphorylation and ATP synthase activity. Consequently, the stressed cells had decreased expression of the genes encoding ATP-dependent amino acid transporters and proteins involved in translation. Other genes up-regulated in response to nitrite include the genes in the Fur regulon, which is suggested to be involved in iron homeostasis, and genes in the Per regulon, which is predicted to be responsible for oxidative stress response.

The sulfate-reducing bacteria represent a group of microorganisms characterized by the ability to use sulfate as an electron acceptor in anaerobic respiration (47). Microbial sulfate reduction by these microorganisms is recognized as a widely distributed process of great ecological importance (29, 54). Historical interest in sulfate-reducing bacteria has been focused on their involvement in biocorrosion of ferrous metals in the petroleum industry and of concrete structures in wastewater collection systems (15, 24). More recent studies (7, 25, 27, 28) have documented the ability of a number of sulfate-reducing bacteria to reduce soluble metal oxyanions to insoluble forms, a process of great potential in the bioremediation of toxic heavy metals and radionuclides such as chromium and uranium (11, 56).

To effectively immobilize heavy metals and radionuclides using sulfate-reducing bacteria, it is important to understand the microbial response to adverse environmental factors common in contaminated subsurface environments. One such factor is the high nitrate concentration of many contaminated sites at the nuclear weapon complexes in the United States managed by the Department of Energy (39, 49). The presence of nitrate may pose a specific stress to sulfate-reducing bacteria as nitrate has been observed to suppress sulfate reduction activity in situ (9, 21). However, it has been suggested that nitrite, an intermediate that transiently accumulates during nitrate reduction (3, 23, 58), is directly responsible for the inhibition of sulfate reduction activity (26, 38). Furthermore, the dissimilatory sulfite reductase, which is a key enzyme in the sulfate reduction pathway, has been implicated in previous reports as the target of nitrite inhibition (13, 16). Consequently, one would predict that energy generation pathways in sulfate-reducing bacteria would be altered upon exposure to nitrite. Thus, it is important to examine the global transcription profiles following nitrite exposure to understand how the complex energy generation pathways in sulfate-reducing bacteria respond to nitrite and to predict the performance of these bacteria for bioremediation.

In this report we used *Desulfovibrio vulgaris* Hildenborough as a model organism to investigate the gene expression profile during the inhibition of sulfate reduction by nitrite. The microbial stress responses at the transcriptional level were studied with whole-genome microarrays. Our results indicate that *D. vulgaris* is capable of rapid nitrite reduction and that the exposure to nitrite triggers a well-coordinated response in

* Corresponding author. Mailing address: Institute for Environmental Genomics and Department of Botany and Microbiology, University of Oklahoma, Norman, OK 73019. Phone: (405) 325-6073. Fax: (405) 325-3442. E-mail: jzhou@ou.edu.

† Supplemental material for this article may be found at http://aem.asm.org/.

‡ http://vimss.lbl.gov.

pathways of energy metabolism, nitrogen metabolism, oxidative stress response, and iron homeostasis.

MATERIALS AND METHODS

Organism and growth conditions. *D. vulgaris* strain Hildenborough (ATCC 29579) was grown in an anaerobic medium containing lactate plus sulfate (LS medium) of the following composition (per liter): 6.72 g of sodium lactate, 7.10 g of Na_2SO_4, 0.963g of anhydrous $MgSO_4$, 1.07 g of NH_4Cl, 0.383 g of K_2HPO_4, 0.088 g of $CaCl_2 \cdot 2H_2O$, 0.620 mg of resazurin, 0.600 g of Na_2CO_3, 25.0 ml of 1 M HEPES [4-(2-hydroxyethyl)-1-piperazineethanesulfonic acid] (pH 7.0), 12.5 ml of a trace mineral solution, 0.75 g of L-cysteine, and 1.0 g of yeast extract. The trace mineral solution contained the following (per liter): 1.0 g of $FeCl_2 \cdot 4H_2O$, 0.3 g of $CoCl_2 \cdot 4H_2O$, 0.5 g of $MnCl_2 \cdot 4H_2O$, 0.2 g of $ZnCl_2$, 20 mg of H_3BO_3, 50 mg of $Na_2MoO_4 \cdot 4H_2O$, and 0.1 g of $NiCl_2 \cdot 6H_2O$. Cysteine was added as a reductant after the medium had been boiled and cooled to room temperature. The headspace of the medium container was continuously flushed with oxygen-free nitrogen gas, and the pH was adjusted to 7.2 ± 0.1 with 5 M NaOH. A vitamin solution (10 ml per liter) (5) was added to the autoclaved medium from filter-sterilized anaerobic stock solutions. Cultures were incubated in the dark at 37°C in stoppered 160-ml serum bottles with 100 ml of LS medium or in 30-ml anaerobic culture tubes with 10 ml of medium and sealed with butyl rubber stoppers and aluminum seals. Strictly anaerobic techniques were used throughout all experimental manipulations.

Oligonucleotide probe design and microarray construction. DNA microarrays covering 3,482 of the 3,531 annotated protein-coding sequences of the *D. vulgaris* genome were constructed with 70-mer oligonucleotide probes (18). Oligonucleotide probes (3,574) were designed to cover all open reading frames (ORFs) for the genome of *D. vulgaris* Hildenborough, using the computer software tool ArrayOligoSelector (4), based on an early version (June 2003) of the gene model with 3,584 ORFs. The specificity of all designed oligonucleotide probes was examined with two criteria, as follows. From a BLAST analysis (1), 496 oligonucleotide probes were considered nonspecific to individual genes if they showed a >85% sequence identity or a >18-base continuous homologous stretch with other ORFs in the genome (18). These nonspecific oligonucleotide probes were redesigned against the genome using two other programs, OligoPicker (60) and OligoArray (51), with the same design parameters. Following the examination of the entire probe set according to the oligonucleotide probe design criteria (18), 3,471 (97.1%) specific oligonucleotide probes were obtained, and 103 (2.9%) remained nonspecific. When this early version gene model was mapped to the published version of the *D. vulgaris* gene model (19), 3,482 of the 3,531 protein-coding sequences were covered with 3,439 specific and 43 nonspecific oligonucleotide probes (see Table S1 in the supplemental material).

All designed oligonucleotides were commercially synthesized without modification by MWG Biotech Inc. (High Point, NC). The concentration of oligonucleotides was adjusted to 100 pmol/μl. Oligonucleotide probes were prepared in 50% (vol/vol) dimethyl sulfoxide (Sigma-Aldrich, St. Louis, MO) and spotted onto UltraGAPS glass slides (Corning Life Sciences, Corning, NY) using a BioRobotics Microgrid II microarrayer (Genomic Solutions, Ann Arbor, MI). Each oligonucleotide probe had two replicates on a single slide. Additionally, six different concentrations (5, 25, 50, 100, 200, and 300 ng/μl) of genomic DNA were also spotted (eight duplicates of each of the six concentrations on a single slide) as additional positive controls. After the oligonucleotide probes were printed, they were fixed onto the slides by UV cross-linking (600 mJ of energy), according to the protocol of the manufacturer of the UltraGAPS glass slides (Corning Life Science, Corning. NY).

Exposure to nitrite stress. In experiments for nitrite stress microarray analysis, *D. vulgaris* cultures were grown to exponential phase (optical density at 600 nm [OD_{600}] of ca. 0.4) in LS medium. To triplicate cultures, nitrite from anaerobic stock solutions was added to a final concentration of 2.5 mM. Cell samples of each culture were harvested immediately after the addition of nitrite, and after 30, 60, 90, 150, and 240 min by centrifugation (5,000 × *g*) for 5 min at 4°C. Cell samples from triplicate control cultures without the addition of nitrite were collected simultaneously at the same time points. Cell pellets were then immediately frozen in liquid N_2 and stored at −80°C prior to RNA isolation. To perform appropriate statistical analysis, cell samples were not pooled in subsequent processing. To prevent organic contamination, all glassware was acid washed and baked at 300°C overnight.

Analytical methods. Growth of cultures was monitored spectrophotometrically (OD_{600}). Nitrite was analyzed on a Dionex DX-120 ion chromatograph apparatus with a PeakNet analysis software package and a Dionex IonPak Anion Exchange column as previously described (17). The mobile phase contained 1.8 mM Na_2CO_3 and 1.7 mM $NaHCO_3$. Peaks were quantified via a conductivity detector, and concentrations were determined using known standards. Samples from the cultures were filtered through 0.20-μm-pore-size filters prior to ion chromatographic analysis.

Total RNA extraction, purification, and labeling. RNA extraction, purification, and labeling were performed independently on each cell sample. Total cellular RNA was isolated using TRIzol Reagent (Invitrogen, Carlsbad, CA) following the manufacturer's protocol. RNA extracts were purified according to the RNeasy Mini Kit (QIAGEN, Valencia, CA) instructions, and on-column DNase digestion was performed with an RNase-free DNase set (QIAGEN, Valencia, CA) to remove genomic DNA contamination, according to the manufacturer's procedure.

To generate cDNA targets with reverse transcriptase, 10 μg of purified total RNA was used for each labeling reaction using a previously described protocol (55). Briefly, random hexamers (Invitrogen) were used for priming, and the fluorophore Cy3-dUTP or Cy5-dUTP (Amersham Biosciences, Piscataway, NJ) was used for labeling. After the labeling, RNA was removed by NaOH treatment, and cDNA was immediately purified with a QIAGEN PCR mini kit. The efficiency of labeling was routinely monitored by measuring the absorbance at 260 nm (for DNA concentration), 550 nm (for Cy3), or 650 nm (for Cy5). Two samples of each total RNA preparation were labeled, one with Cy3-dUTP and another with Cy5-dUTP, for microarray hybridization.

Microarray hybridization, washing, and scanning. To hybridize microarray glass slides, the Cy5-dUTP-labeled cDNA targets from one nitrite-treated culture were mixed with the Cy3-dUTP-labeled cDNA targets from one untreated control culture and vice versa (dye swap). As a result, each biological sample was hybridized to two microarray slides. Equal amounts of Cy3- or Cy5-labeled probes were mixed and resuspended in 35 to 40 μl of hybridization solution that contained 50% (vol/vol) formamide, 5× saline-sodium citrate (5× SSC; 1× SSC is 150 mM NaCl plus 15 mM sodium citrate, pH 7.0), 0.1% (wt/vol) sodium dodecyl sulfate (SDS), and 0.1 mg of herring sperm DNA/ml (Invitrogen). The hybridization solution was incubated at 95 to 98°C for 5 min, centrifuged to collect condensation, kept at 50°C, and applied onto microarray slides. Hybridization was carried out in hybridization chambers (Corning Life Sciences, Corning, NY) at 45°C overnight (16 to 20 h). A total of 10 μl of 3× SSC solution was added to the wells at both ends of the microarray slides to maintain proper chamber humidity and probe hydration around the edges of the coverslips. Microarray slides were washed according to the instructions for spotted oligonucleotide microarrays on UltraGAPS slides by the manufacturer (Corning) in the following steps: two washes in a solution containing 2× SSC and 0.1% (wt/vol) SDS at 42°C at 5-min intervals, two washes in a solution containing 0.1× SSC and 0.1% (wt/vol) SDS at room temperature at 10-min intervals, and two washes in 0.1× SSC at room temperature at 2-min intervals. After being blown dry by a stream of N_2, the slides were scanned for the fluorescence intensity of both the Cy5 and Cy3 fluorophores using a ScanArray Express microarray analysis system (Perkin Elmer, Boston, MA).

Image quantification and data analysis. To determine signal fluorescence intensities for each spot, 16-bit TIFF scanned images were analyzed by application of the software ImaGene, version 6.0 (Biodiscovery, Marina Del Rey, Calif.) to quantify spot signal, spot quality, and background fluorescence intensities. Empty spots, poor spots, and negative spots were flagged according to the instruction of the software and removed in subsequent analysis (12).

The resulting data files were subjected to Lowess intensity-based normalization and further analyzed using GeneSpring, version 5.1 (Silicon Genetics, Redwood City, Calif.). Lowess normalization was performed on each microarray slide, and results of the triplicate cultures from the same time point were used for statistical analysis. To assess the statistical significance of individual data points, a Student *t* test was used to calculate a *P* value to test the null hypothesis that the expression level was unchanged. A statistical model incorporating both per gene variance and operon structure was further used to compute the posterior probability that each gene changed its expression level in the direction indicated by its mean value (48). An average linkage hierarchical clustering analysis of the time course transcriptional response to nitrite stress with the Euclidean distance as the similarity metric was performed and visualized with Hierarchical Clustering Explorer, version 3.0 (53).

The expression of genes encoding iron-containing proteins was evaluated by comparing the expression levels of transcripts coding for iron-containing proteins to the average values for all genes in the cell. To identify genes encoding iron-containing proteins, we examined domain structure as predicted by InterPro, version 9.0 (37), and included all genes with domains annotated as binding iron.

Real-time quantitative RT-PCR analysis. To independently validate gene expression results from the microarray analysis, eight ORFs exhibiting a range of expression levels from low to high (as identified by microarray analysis) were chosen for analysis using real-time reverse-transcription PCR (RT-PCR). Primer

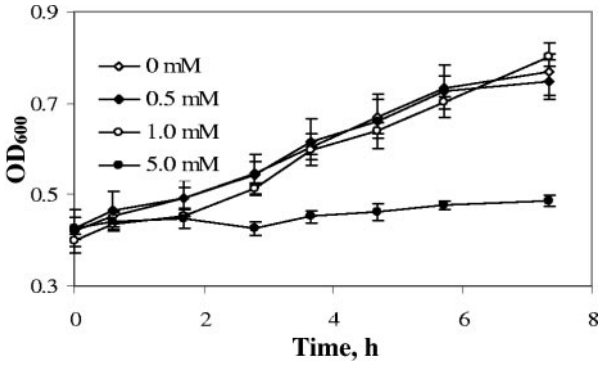

FIG. 1. Impact of nitrite on the growth of *D. vulgaris*. Nitrite of different concentrations was added to sulfate-reducing bacterial cultures in mid-log phase, and growth was subsequently monitored as the OD_{600}. Data are averaged from triplicate cultures, with error bars indicating standard deviations.

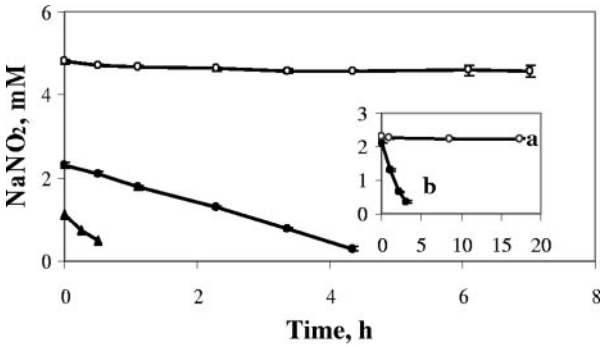

FIG. 2. Nitrite reduction by *D. vulgaris* cultures. Following the addition of various initial concentrations of nitrite into mid-log-phase cultures (OD_{600}, 0.4), reduction of nitrite was monitored over time. (Inset) Changes in nitrite concentration in the presence of 40 mM sulfide but no cells (a) and mid-log cells (OD_{600}, 0.4) only (b). Axis labels in the inset are the same as in the main figure. Results shown are averages of triplicates, with error bars indicating standard deviation.

pairs (in parentheses, forward and reverse, respectively) were designed for the following genes to yield products of ~100 bp (52): DVU0625, encoding a cytochrome *c* nitrite reductase (5′-AGAACCTCTGGCTCGGCTAT and 5′-CGATTGATACGGTCGATGTG); DVU0942, encoding a Fur family transcriptional regulator (5′-CATCGCCGTATTTCAGGATT and 5′-GAGATGCCCGCCTACTTTC); DVU1290, encoding the gamma subunit of a putative nitrate reductase (5′-TTTCCGGCTTTCAGTACGTT and 5′-AGACTTGGCCCAATCCACTA); DVU1574, encoding a ribosomal protein L25 (5′-GGTGGCAAGCTCGAAGTCTA and 5′-GATGTCGAGTTCGGTCAGGT); DVU2247, encoding an AhpC/Tsa family antioxidant (5′-TCTATCCGCTGGACTTCACC and 5′-ACACCGATGACCTC GACATT); DVU2543, encoding a hybrid cluster protein (5′-ACCTCACCATCTACGCCTTG and 5′-GCTTTGGCCGTGTATTCATC); DVU2571, encoding a ferrous iron transport protein B (5′-GAAGGAGGTCATCGTCTCCA and 5′-GGGGTCGTTCCTGATCTGT); and DVU2680, encoding a flavodoxin (5′-CTTCAT and 5′-CCCGCAGAAGTACTCGTAGG).

The RT-PCR analysis was carried out using a previously described protocol (59). Briefly, the cDNA template for real-time RT-PCR was synthesized from 5 μg of total RNA using the reverse transcriptase reaction with random hexamer priming (Invitrogen). The quantitative PCR was carried out in an iCycler thermal cycler (Bio-Rad, Hercules, Calif.) that measured the increases in fluorescence resulting from the incorporation of SYBR green dye (Molecular Probes, Eugene, Oreg.) into double-strand DNA. Real-time data acquisition and analysis were performed with the software iCycle 2.3, version B, according to the manufacturer's instructions. Standards for each gene of interest were obtained by serial dilutions of PCR amplification product from *D. vulgaris* genomic DNA using the procedure described above but without SYBR green dye. The standards were used to establish a standard curve consisting of seven points serially diluted from 10^7 to 10^1 copies. Copy numbers of the target gene transcripts were determined by comparison with the standard curves, and then gene expression differences between the treatment and control samples were determined.

RESULTS

Growth inhibition of *D. vulgaris* by nitrite. The inhibitory effect of nitrite on the growth of *D. vulgaris* was evaluated by adding different concentrations of nitrite to actively growing cultures (OD_{600} of ca. 0.4). No significant growth inhibition was observed with nitrite concentrations below 1 mM, as the growth curves overlapped between nitrite-treated cultures and control cultures (Fig. 1). When 2.5 mM nitrite was added to the medium, a slower growth rate was observed. When the nitrite concentration was increased to 5 mM, the growth of *D. vulgaris* was significantly decreased, and no change in OD was observed over the monitored time (Fig. 1).

Reduction of nitrite by *D. vulgaris*. To further determine the connection between nitrite and the growth inhibition of *D. vulgaris*, nitrite levels were monitored in the *D. vulgaris* cultures (Fig. 2). Abiotic reduction of nitrite by the medium or sulfide was excluded as nitrite was stable in the presence of 40 mM sulfide but no cells in the controls. On the other hand, with initial concentrations lower than 2.5 mM, nitrite decreased rapidly in active *D. vulgaris* cultures, indicating that nitrite was reduced by *D. vulgaris* cells. In contrast, *D. vulgaris* cultures were unable to reduce 5 mM nitrite, which coincided with nearly complete inhibition of growth, as shown in Fig. 1.

Transcriptome analysis of nitrite stress. To examine the nitrite stress response in *D. vulgaris*, microarray experiments were carried out to compare global gene expression profiles between nitrite-stressed *D. vulgaris* cultures and control cultures without nitrite exposure (see Table S2 in the supplemental material). In order to achieve an optimal stress response, *D. vulgaris* cells were challenged by a sublethal nitrite level (2.5 mM), which effectively inhibited cell growth but still allowed active reduction of nitrite (Fig. 2). Because tolerance to nitrite was found to be dependent on the biomass concentration at the time of nitrite addition (16), cultures of similar optical densities (OD_{600} of ca. 0.4) were used throughout the study.

Significant changes in gene expression profiles occurred within 30 min following nitrite addition and peaked at 60 min, with 330 genes up-regulated and 273 genes down-regulated (Fig. 3) more than twofold. Subsequently, transcriptional responses rapidly diminished with only 82 genes still up-regulated and 86 genes down-regulated more than twofold 4 h after nitrite addition (Fig. 3). Concurrently, the initial 2.5 mM nitrite concentration dropped below 0.5 mM. The steady decline in transcriptional response subsequent to its peaking at 60 min mirrored the time course of reduction of nitrite by *D. vulgaris*. These results indicated a correlation between the dynamics of transcriptional response and the reduction of nitrite between 60 min to 240 min.

To illustrate the gene functions involved in the nitrite stress response, genes with altered expression levels after 1 h of nitrite exposure were grouped into functional role categories according to the annotation of The Institute for Genomic Research (TIGR) of the *D. vulgaris* Hildenborough genome sequence (19, 45), as shown in Fig. 4. Notably, a large portion of the highly up-regulated genes were grouped into cellular roles

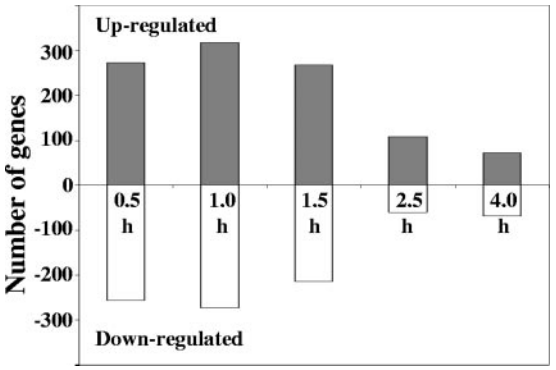

FIG. 3. Temporal profiling of the transcriptional response to sodium nitrite by *D. vulgaris*. Each column represents the number of genes showing significant changes ($P < 0.05$) in gene expression level versus time elapsed following the addition of nitrite. Positive and negative values indicate up- and down-regulation, respectively.

involved in regulatory functions, signal transduction, and organic acid oxidation including genes encoding the L-lactate dehydrogenase, formate dehydrogenase, and pyruvate ferredoxin oxidoreductase, suggesting a shift in energy flow through complex regulatory pathways when *D. vulgaris* cells sense the presence of nitrite. On the other hand, many of the highly down-regulated genes have functions in protein biosynthesis and encode transport and binding proteins, perhaps indicating a slowdown in normal cellular biosynthetic activities when challenged by nitrite stress.

Validation of microarray results. To validate transcriptional results generated by microarray hybridization, real-time RT-PCR analysis was conducted to quantify the expression levels of eight genes (see Fig. S1 in the supplemental material). A high degree of correlation was observed between results from microarray analy-

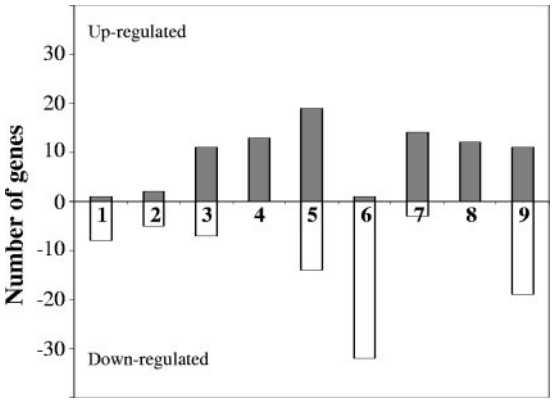

FIG. 4. Functional profiling of the transcriptional response by *D. vulgaris* 1 h following 2.5 mM sodium nitrite addition. The functional role category annotation is that provided by TIGR (www.tigr.org). Each column represents the number of genes in a selected functional category showing significant changes in mRNA abundance in response to nitrite. Positive and negative values indicate up-and down-regulation, respectively. Columns: 1, amino acid biosynthesis; 2, biosynthesis of cofactors, prosthetic groups, and carriers; 3, cell envelope; 4, cellular processes; 5, energy metabolism; 6, protein synthesis; 7, regulatory functions; 8, signal transduction; and 9, transport and binding proteins. Shown are selected role categories with highly differentially expressed genes (change of more than threefold).

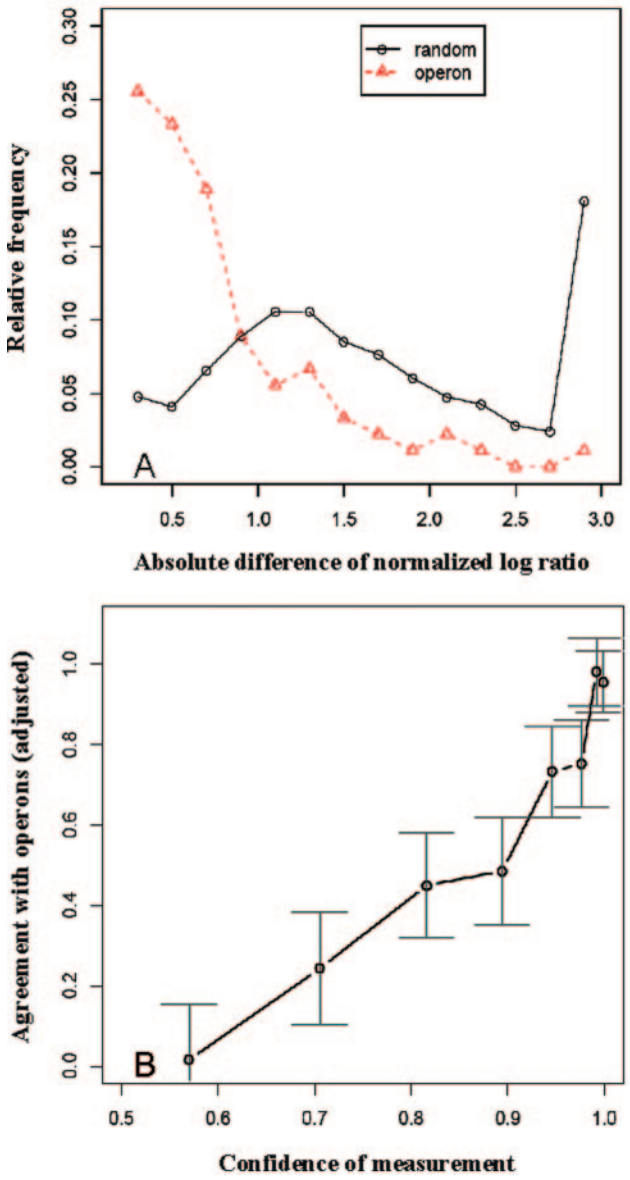

FIG. 5. Validation of microarray results by computational approaches. (A) Log ratio expression difference of gene pairs within the same operon versus gene pairs selected at random. The normalized frequency was plotted against the ratio expression difference between the treatments and control. Genes within the same operon responded more similarly than genes randomly selected from the genome under sodium nitrite exposure. (B) Agreement within predicted operons at the 90-min time point. All genes were divided into eight groups based on the confidence level of the measured change computed by the OpWise program (http://www.microbesonline.org/OpWise). A confidence of 0.5 indicates complete uncertainty as to whether the gene was up- or down-regulated, while a value of 1 indicates certainty that the measured change in mean reflects the actual direction of change. The *y* axis shows the fraction of genes (above that expected by chance) in each group that changed in the same direction as adjacent genes predicted to be in the same operon, together with 95% confidence intervals for the estimate. Values near 1 indicate perfect agreement with all co-operonic genes changing in the same direction, while values near 0 indicate the level of agreement expected by chance (i.e., 50%).

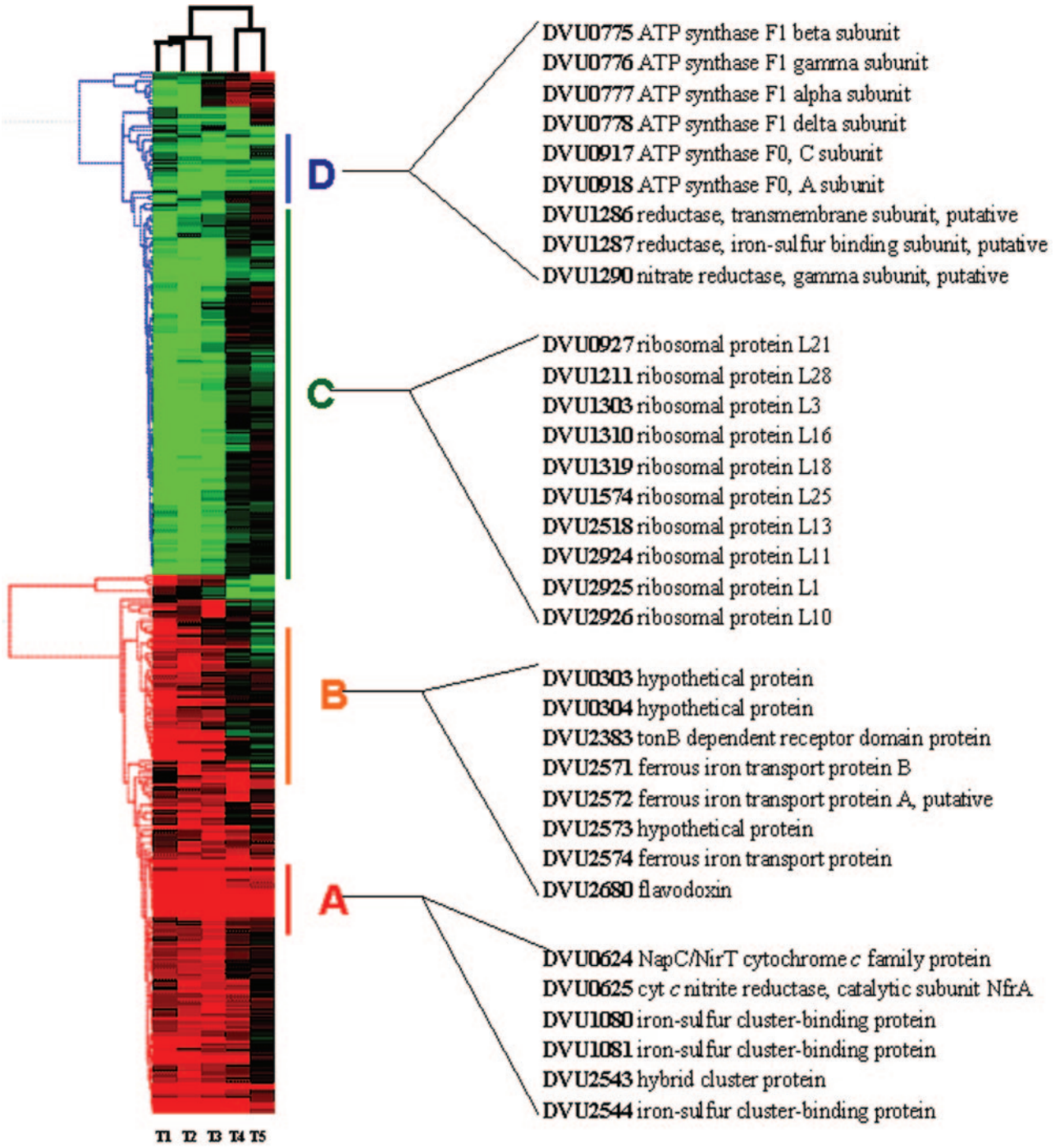

FIG. 6. Hierarchical clustering of selected genes with significant changes ($P < 0.05$ and a change of more than twofold at least at one time point) in expression in response to 2.5 mM nitrite. Red indicates up-regulation, whereas green represents repression. Each row represents the expression of a single gene, and each column represents an individual time point following nitrite addition: T1, 0.5 h; T2, 1.0 h; T3, 1.5 h; T4, 2.5 h; and T5, 4.0 h. Listed genes are examples from each cluster. Cluster A consists of genes highly induced throughout the duration of the experiment; cluster B consists of genes highly induced within 1.5 h of the addition of nitrite but for which induction diminished or even reversed subsequently; cluster C consists of genes repressed during the early response to nitrite but for which repression was later alleviated; and cluster D consists of genes down-regulated throughout the experiment.

sis and RT-PCR ($r^2 = 0.93$), as reported in previous studies that used this microarray procedure (12, 59), thus affirming the accuracy of this approach in the current study.

In addition to real-time RT-PCR analysis, expression differences for gene pairs within the same predicted operon or gene pairs selected at random were compared to determine whether changes observed in microarray experiments were authentic (12). Consistent with our expectation (Fig. 5A), genes within

TABLE 1. Effect of nitrite exposure on the transcriptional responses of *D. vulgaris* genes involved in energy metabolism

Gene identifier and response	Annotation	Expression ratio (treatment/control) at time point[a]:				
		0.5 h	1.0 h	1.5 h	2.5 h	4.0 h
Up-regulation						
DVU0172	Iron-sulfur cluster-binding protein	3.0	2.8	1.8	0.50	0.31
DVU0173	Thiosulfate reductase; putative	2.5	1.9	1.5	0.55	0.45
DVU0600	L-Lactate dehydrogenase (Ldh)	2.1	1.8	1.9		
DVU0624	NapC/NirT cytochrome *c* family protein	13.5	11.4	12.2	9.4	11.4
DVU0625	Cytochrome *c* nitrite reductase; catalytic subunit NfrA; putative	18.5	12.8	14.9	7.5	5.7
DVU1080	Iron-sulfur cluster-binding protein	54.2	81.8	58.6	28.7	27.2
DVU1081	Iron-sulfur cluster-binding protein	12.6	10.5	12.5	6.8	7.2
DVU1569	Pyruvate ferredoxin oxidoreductase; alpha subunit (PorA)	—	2.0	2.3	—	—
DVU1570	Pyruvate ferredoxin oxidoreductase; beta subunit (PorB)	—	2.2	2.3	—	—
DVU2524	Cytochrome c_3; putative	2.2	3.4	5.0	—	—
DVU2525	Periplasmic [NiFe] hydrogenase; small subunit; isozyme 2 (HynB-2)	—	1.5	1.6	—	—
DVU2526	Periplasmic [NiFe] hydrogenase; large subunit; isozyme 2 (HynA-2)	8.1	9.1	9.5	4.7	3.2
DVU2543	Hybrid cluster protein	27.5	34.5	65.1	82.7	37.3
DVU2544	Iron-sulfur cluster-binding protein	39.8	50.7	82.0	233.0	30.3
DVU2810	Formate dehydrogenase formation protein FdhE; putative	1.5	—	1.5	1.8	—
DVU2811	Formate dehydrogenase; beta subunit; putative	—	—	2.1	2.8	—
DVU2812	Formate dehydrogenase; alpha subunit; selenocysteine-containing (FdnG-3)	—	—	1.8	—	—
DVU3261	Fumarate reductase; cytochrome *b* subunit (FrdC)	2.0	3.5	3.2	—	—
DVU3262	Fumarate reductase; flavoprotein subunit (FrdA)	1.8	2.9	2.6	—	1.4
DVU3263	Fumarate reductase; iron-sulfur protein (FrdB)	1.9	3.7	3.1	—	—
Down-regulation						
DVU0431	Ech hydrogenase; subunit EchD; putative	0.37	0.53	—	—	—
DVU0432	Ech hydrogenase; subunit EchC; putative	0.41	0.51	0.59	—	—
DVU0433	Ech hydrogenase, subunit EchB; putative	0.49	0.59	—	—	—
DVU0434	Ech hydrogenase, subunit EchA; putative	0.57	0.59	—	—	—
DVU0774	ATP synthase; F_1 epsilon subunit (AtpC)	—	0.42	0.39	0.46	—
DVU0775	ATP synthase; F_1 beta subunit (AtpD)	—	0.31	0.32	0.30	—
DVU0776	ATP synthase; F_1 gamma subunit (AtpG)	—	0.30	0.42	0.18	—
DVU0777	ATP synthase, F_1 alpha subunit (AtpA)	0.40	0.31	0.23	0.24	—
DVU0778	ATP synthase; F_1 delta subunit (AtpH)	0.48	0.31	0.38	0.25	—
DVU0779	ATP synthase; F_0 B subunit; putative (AtpF2)	0.57	0.38	0.36	0.40	—
DVU0780	ATP synthase; F_0 B subunit; putative (AtpF1)	0.44	0.40	0.40	—	—
DVU0917	ATP synthase; F_0 C subunit (AtpE)	—	0.37	0.29	0.31	0.59
DVU0918	ATP synthase; F_0 A subunit (AtpB)	0.46	0.37	0.29	0.42	0.67
DVU1286	Reductase; transmembrane subunit; putative (DsrP)	0.34	0.33	0.24	0.56	—
DVU1287	Reductase; iron-sulfur binding subunit; putative (DsrO)	0.19	0.19	0.17	0.54	—
DVU1288	Cytochrome *c* family protein (DsrJ)	0.19	0.21	0.23	0.43	—
DVU1289	Reductase; iron-sulfur binding subunit; putative (DsrK)	0.15	0.19	0.22	0.47	—
DVU1290	Nitrate reductase; gamma subunit; putative (DsrM)	0.16	0.17	0.17	0.53	—
DVU1769	Periplasmic [Fe] hydrogenase; large subunit (HydA)	—	0.59	0.38	—	0.38
DVU1770	Periplasmic [Fe] hydrogenase; small subunit (HydB)	0.55	0.42	0.24	0.25	0.21
DVU2792	Electron transport complex protein RnfC; putative	0.43	0.33	0.42	0.47	0.50
DVU2793	Electron transport complex protein RnfD; putative	0.58	0.36	0.59	0.47	0.54
DVU2794	Electron transport complex protein RnfG; putative	0.51	0.36	0.49	0.43	0.51
DVU2795	Electron transport complex protein RnfE; putative	—	0.40	—	0.48	—
DVU2796	Electron transport complex protein RnfA; putative	—	0.47	0.61	0.56	0.61
DVU2797	Iron-sulfur cluster-binding protein	—	0.42	—	0.62	—
DVU2798	ApbE family protein	0.58	0.41	0.53	0.62	—

[a] Changes of gene expression level at different time points following addition of 2.5 mM sodium nitrite to cultures compared to controls without nitrite addition. Expression levels were obtained at the same time points from both the treatment and control cultures for the calculation of the expression changes resulting from the stressor. Expression ratio values greater than 1 denote increases in gene expression and values between 0 and 1 indicate decreases in gene expression ($P < 0.05$). Dashes indicate that no significant change in gene expression was observed.

the same operon responded more similarly than genes randomly selected from the genome. As shown in Fig. 5A, the within-operon pairs had higher probabilities to exhibit much smaller log ratio differences than gene pairs chosen at random, thus confirming the agreement between microarray results and operon prediction and the high quality of the expression data. Furthermore, a second operon-based computational method was also used to test the validation of the microarray results through evaluation of the confidence levels of gene expression (48). Consistently, genes identified as having confident changes in expression were in agreement with other genes found in the same operon (Fig. 5B). Thus, the comparison with operon structure confirmed both the high quality of the expression data and our ability to identify reliable data points.

Hierarchical clustering analysis of temporal gene expression profile. To identify differential gene expression patterns in

TABLE 2. Effect of nitrite exposure on the transcriptional responses of *D. vulgaris* genes involved in nitrogen metabolism

Gene identifier	TIGR annotation	Expression ratio (treatment/control) at time point[a]:				
		0.5 h	1.0 h	1.5 h	2.5 h	4.0 h
DVU0095	Polyamine ABC transporter, periplasmic polyamine-binding protein	0.24	0.19	0.21	—	—
DVU0105	Glutamine ABC transporter; ATP-binding protein	0.30	0.47	0.59	—	—
DVU0106	Glutamine ABC transporter; permease protein	0.64	0.64	0.62	—	—
DVU0107	Glutamine ABC transporter; periplasmic glutamine-binding protein	0.40	0.30	0.39	—	—
DVU0388	Amino acid ABC transporter; ATP-binding protein	0.25	0.19	0.28	—	—
DVU0624	NapC/NirT cytochrome *c* family protein	13.5	11.4	12.2	9.4	11.4
DVU0625	Cytochrome *c* nitrite reductase; catalytic subunit NfrA; putative	18.5	12.8	14.9	7.5	5.7
DVU0751	Amino acid ABC transporter; permease protein; His/Glu/Gln/Arg/opine family	0.50	0.39	0.42	0.53	0.45
DVU0752	Amino acid ABC transporter; amino acid-binding protein	0.49	0.25	0.33	0.28	0.27
DVU0966	Amino acid ABC transporter, periplasmic amino acid-binding protein	0.40	0.17	0.17	0.38	0.27
DVU0967	Amino acid ABC transporter; permease protein; His/Glu/Gln/Arg/opine family	0.47	0.40	0.56	—	—
DVU0968	Amino acid ABC transporter, ATP-binding protein	0.32	0.38	0.36	—	—
DVU1026	Uracil permease	0.14	0.21	0.30	—	0.47
DVU1237	Amino acid ABC transporter; permease protein; His/Glu/Gln/Arg/opine family	0.28	0.61	0.41	—	—
DVU1238	Amino acid ABC transporter; periplasmic amino acid-binding protein	0.39	0.62	0.32	—	0.47
DVU1766	Aspartate ammonia-lyase; putative	0.53	0.49	0.36	0.51	0.53
DVU2113	Xanthine/uracil permease family protein	0.23	0.28	0.31	—	0.54
DVU2242	Asparaginase family protein	0.64	0.58	0.50	—	—
DVU2543	Hybrid cluster protein	27.5	34.5	65.1	82.7	37.3
DVU3392	Glutamine synthetase type I	1.5	2.2	2.8	2.2	1.6

[a] See footnote to Table 1.

the nitrite stress response by *D. vulgaris*, a hierarchical clustering analysis was conducted on the transcriptional profile (Fig. 6). Cluster A consists of genes highly induced throughout the duration of the experiment, including the operon encoding the nitrite reductase and several redox-active proteins. Notably, the gene for the hybrid cluster protein was highly up-regulated in response to the presence of nitrite, providing more evidence for its suggested role in nitrogen metabolism (57, 63). Cluster B represents a group of genes highly induced within 1.5 h of the addition of nitrite but for which the induction diminished or even reversed subsequently. Interestingly, genes included in this cluster encode ferrous iron transport proteins, suggesting a role of iron homeostasis in the initial stress response to nitrite. Cluster C covers a large number of genes repressed during the early response to nitrite that were later restored to expression levels observed in the control cultures. Within Cluster C, genes for ribosomal proteins were particularly in abundance, consistent with prior findings of an early slowdown in protein synthesis (Fig. 4). Cluster D is comprised of genes down-regulated throughout the experiment's duration, including genes that have functions in energy metabolism. From the concurrent induction of genes in nitrite reduction (cluster A) and the repression of genes encoding ATP synthase subunits (cluster D), we hypothesize that electron flow was likely shifted from respiratory phosphorylation to the reduction of nitrite.

Genes involved in energy metabolism. Genes having functions in energy metabolism exhibited considerable divergence in their transcriptional response to nitrite (Table 1). In contrast to the severe repression of ATP synthase genes, genes encoding the membrane-bound lactate dehydrogenase (*ldh*) and pyruvate ferredoxin oxidoreductase (*porAB*) were induced, pointing to potential increases in substrate level phosphorylation and electron flow. In parallel, a number of operons encoding redox proteins participating in periplasmic electron transfer were also up-regulated, including the gene encoding the periplasmic [NiFe] hydrogenase (*hynBA-2*) and its putatively associated tetraheme cytochrome (DVU2524-2526) and one encoding a formate dehydrogenase (DVU2810-2812). Thus, the possibility exists that these redox protein complexes are involved in electron transfer to nitrite or in the turnover of reduced electron carriers, allowing a greater rate of substrate oxidation for substrate level phosphorylation. Additionally, the fumarate reductase operon (*frdABC*) was

TABLE 3. Effect of nitrite exposure on the transcriptional responses of *D. vulgaris* genes in the predicted Fur regulon[a]

Gene identifier	TIGR annotation	Expression ratio (treatment/control) at time point[b]:				
		0.5 h	1.0 h	1.5 h	2.5 h	4.0 h
DVU0763	GGDEF domain protein	11.9	2.1	—	—	—
DVU2378	Transcriptional regulator; AraC family	4.3	4.1	2.4	—	—
DVU2574	Ferrous iron transport protein; putative FeoA	3.5	5.0	3.9	—	—
DVU2680	Flavodoxin	27.6	22.6	4.9	—	—
DVU3330	Conserved hypothetical protein	2.3	5.7	2.3	—	—
DVU0273	Conserved hypothetical protein	15.3	5.2	1.8	—	0.46
DVU0304	Hypothetical protein	34.0	10.1	3.7	—	—

[a] Predicted Fur-binding sites (50).
[b] See footnote to Table 1.

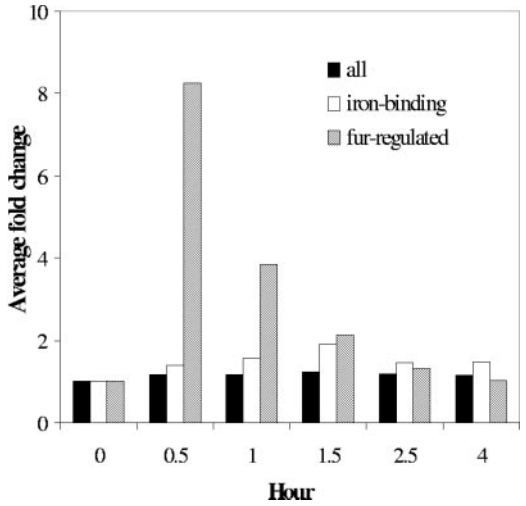

FIG. 7. Average changes in expression levels of selected *D. vulgaris* gene groups following 2.5 mM sodium nitrite addition, with "all" representing all genes covered by the microarray, "iron-binding" representing genes encoding iron-containing proteins, and "fur-regulated" representing genes belonging to the predicted Fur regulon (50).

induced, possibly allowing fumarate to serve as an alternative electron acceptor (Table 1).

Among genes involved in the sulfate reduction pathway, the operon for the triheme cytochrome *c*-containing membrane-bound oxidoreductase (*dsrMKJOP*), which has been implicated as having a role in electron transfer for sulfite reduction (16), was considerably down-regulated in response to nitrite. Two other operons with unknown functions, one encoding the membrane-bound decaheme electron transport complex (*rnfABCDEFG*) and the other for the membrane-bound cytoplasmically oriented Ech hydrogenase (*echABCD*), were also significantly down-regulated.

Genes with functions in nitrogen metabolism. One important observation in response to nitrite was the down-regulation of multiple genes encoding ATP-binding ABC-transporters for amino acids and polyamines (Table 2). With the down-regulation of genes in the sulfate reduction pathway and oxidative phosphorylation (Table 1), the decrease in the expression of energy-dependent transport systems could be linked to the lowered expression of genes involved in energy production in the cells under nitrite stress. The reduced expression of genes for amino acid transporters could also be a result of the down-regulation of genes encoding the protein biosynthetic machinery.

Paradoxically, the glutamine synthetase gene (DVU3392), which participates in nitrogen assimilation (31), was induced during nitrite stress (Table 2). This might result from the increased flux of carbon needed to support substrate level phosphorylation that could spill over into the tricarboxylic acid cycle, increasing the ratio of α-ketoglutarate to glutamine, a possible signal for nitrogen limitation. Additionally, genes encoding the aspartate ammonia-lyase (DVU1766) and asparaginase (DVU2242), which are responsible for the catabolism of amino acids acquired from the medium, were down-regulated (Table 2). Thus, the transition from respiration of sulfate to alternative energy sources could possibly influence the expression profile of genes that participate in the overall carbon and nitrogen metabolism of the cells.

Genes in the predicted Fur regulon. Among the highly induced genes during nitrite stress are ferrous iron transporter genes (Fig. 6), which were predicted to be controlled by the ferric uptake regulator (Fur) at the transcriptional level (50). Interestingly, all genes in the predicted Fur regulon (50) were highly up-regulated for 1.5 h following the onset of nitrite stress (Table 3). Since the Fur regulons of many bacteria are known to be derepressed by iron deficiency (10, 14), induction of the Fur regulon in nitrite stress implies a link between this stress and iron depletion. Indeed, genes encoding iron-containing proteins, including nitrite reductase, were on average up-regulated in response to nitrite (Fig. 7), potentially resulting in a higher demand for iron. It is thus suggested that the highly induced Fur-regulated genes, which include ferrous iron transporters, served as a response to the higher expression of genes of iron-containing proteins.

Genes belonging to the predicted PerR regulon. Because reactive nitrogen species have been shown to trigger oxidative stress responses (36, 41), expression levels of genes predicted to be regulated by the oxidative stress regulator PerR (50) were examined (Table 4). All genes in the PerR regulon were moderately up-regulated at one or more sampling points during the experiment, suggesting that the oxidative stress response is a derivative from nitrite stress.

DISCUSSION

The sulfate-reducing bacteria are of great potential in the bioremediation of heavy metals and radionuclides in anaerobic environments (56, 61). Therefore, considerable research efforts using physiological and genetic approaches have been made to understand the response of these bacteria to unfavorable environmental factors. One significant finding from previous studies is the inhibition of sulfate reduction by nitrite, an

TABLE 4. Effect of nitrite exposure on the transcriptional responses of *D. vulgaris* genes in the predicted PerR regulon[a]

Gene identifier	TIGR annotation	Expression ratio (treatment/control) at time point[b]:				
		0.5 h	1.0 h	1.5 h	2.5 h	4.0 h
DVU0772	Hypothetical protein	1.8	2.4	2.6	2.1	—
DVU2247	Antioxidant; AhpC/Tsa family	3.0	3.1	2.1	1.8	—
DVU2318	Rubrerythrin; putative	—	—	1.5	—	0.53
DVU3095	Transcriptional regulator; Fur family; PerR	—	—	—	2.2	—
DVU3096	Hypothetical protein	—	1.8	—	—	—

[a] Predicted PerR-binding sites are from reference 50.
[b] See footnote to Table 1.

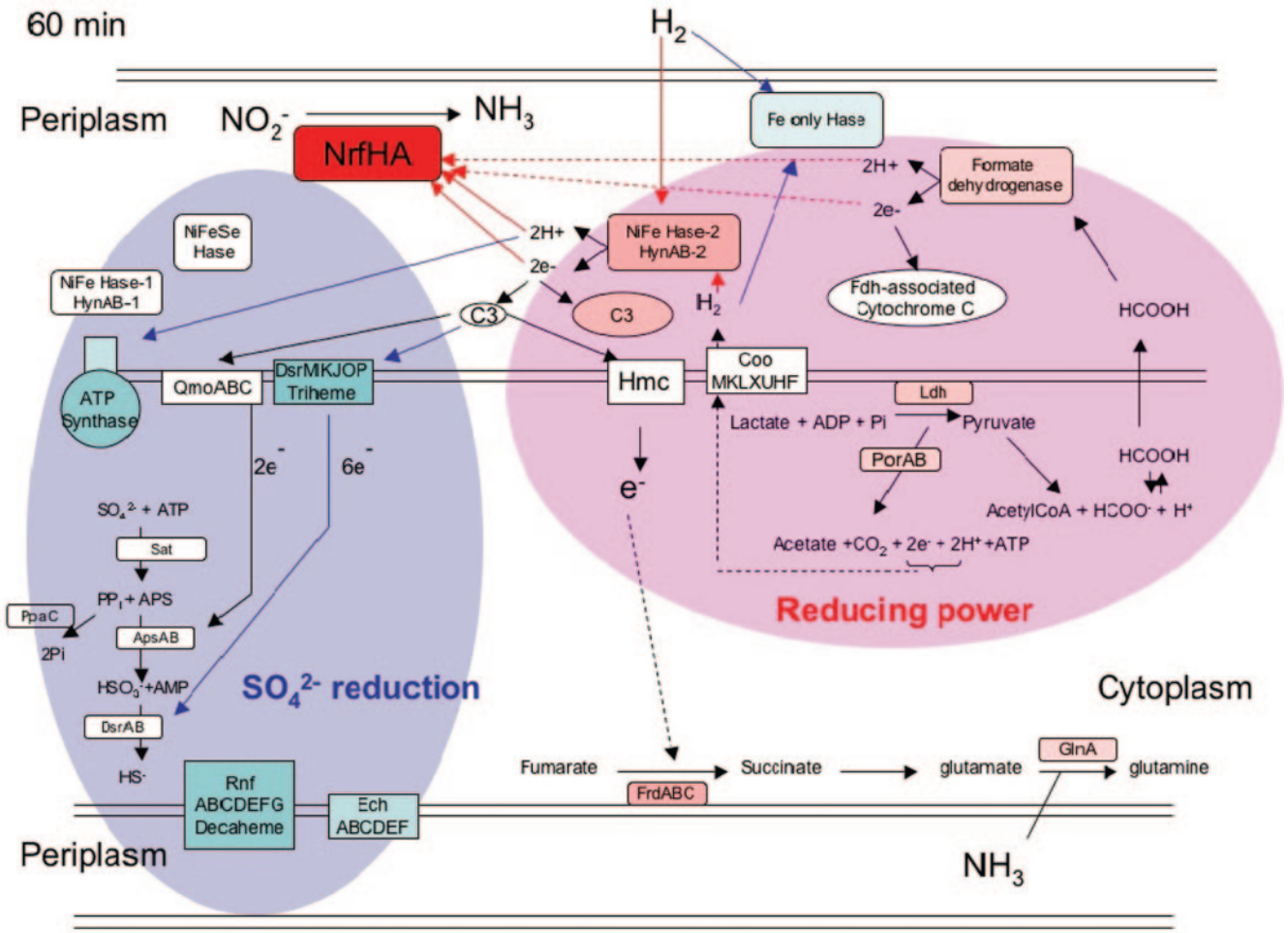

FIG. 8. Conceptual model of the transcriptional responses in the energy metabolism pathways to nitrite stress (2.5 mM $NaNO_2$) by *D. vulgaris* based on the transcriptional profile obtained 60 min after stress exposure. The repression of genes encoding the *dsrMKJOP* triheme transmembrane complex by nitrite suggests that reducing equivalents derived from lactate oxidation were shifted to nitrite reduction. Red designates up-regulation and blue designates down-regulation; changes in the intensity of the red or blue represent the extent of the up- or down-regulation, respectively; white indicates no change detected in expression level.

important intermediate during microbial nitrate reduction (20, 40, 44). The availability of the genome sequence of *D. vulgaris* makes it possible to study stresses at the whole-genome level (19). Using global transcriptional analysis, this work revealed that *D. vulgaris* cells responded to the presence of nitrite with a series of well-coordinated regulatory pathways linking energy metabolism, nitrogen metabolism, iron homeostasis, and oxidative stress response.

Physiological and transcriptional analyses demonstrated that nitrite reduction was the primary mechanism for detoxification by *D. vulgaris* (Fig. 2 and Table 2), which is consistent with previous observations (13). A significant increase in the expression of the nitrite reductase genes reported here (Table 2) was also seen by Haveman et al. (16). However, earlier reports measuring the specific activity of nitrite reductase indicated that the enzyme was essentially constitutive (32) or that activity was actually less in cells exposed to nitrite (44). This disparity has not yet been resolved here and requires further examination.

Major effects on energy generation pathways were expected from the biochemical studies that demonstrated nitrite inhibition of sulfite reductase (16, 62) and the periplasmic [Fe] hydrogenase of *D. vulgaris* (44). Furthermore, as nitrite reduction in the periplasm consumes electrons and protons that are central to respiration, one would expect changes in energy metabolism. Indeed, a number of genes with important roles in energy metabolism were differentially expressed, suggesting the extensive response to nitrite stress in the energy metabolism pathways at the transcriptional level (Table 1), which is illustrated in the proposed conceptual model of the transcriptional responses in the energetics of nitrite reduction (Fig. 8). *D. vulgaris* cells could respond to this energy requirement by the up-regulation of *ldh* and *porAB*, thus increasing the electron flow and the opportunity for substrate level phosphorylation. Simultaneously, the triheme cytochrome *c* (*dsrMKJOP*) operon, which has been suggested to transfer electrons to the sulfite reductase (16), was significantly down-regulated. These results are in good agreement with the earlier work of Haveman et al. (16), who showed the repressive effects of nitrite on

sulfate reduction including sulfate adenylyl transferase and pyrophosphatase.

Interestingly, earlier work on the effects of nitrite on the growth of *D. vulgaris* on lactate- or sulfate-containing medium reported a large accumulation of hydrogen (44). Thus, some of the excess reductant may be channeled to hydrogen production, consistent with the up-regulation of the [NiFe] hydrogenase (isozyme-2) gene. Additionally, the up-regulation of the genes in the fumarate reductase operon (*frdBAC*) (Table 1) could signal the use of fumarate as a terminal electron acceptor in the absence of sulfate/sulfite reduction. Taken as a whole, the repression of sulfate reduction, the increase in nitrite reduction, and the inhibition of [Fe] hydrogenase likely contribute to a diminished proton motive force, which in turn may be responsible for the repression of genes encoding the ATP synthase subunits (Table 1). The resulting slowdown in growth might also reflect the down-regulation of genes for ribosomal proteins and those for the biosynthesis of amino acids during nitrite stress (Fig. 6).

Notably, while the [NiFe] hydrogenase isozyme-2 gene was up-regulated under nitrite stress, the [Fe] hydrogenase gene was down-regulated (Table 1). Currently, the physiological roles of the various hydrogenases in *D. vulgaris* are still not clear. However, the [NiFe] hydrogenase is apparently more suited to functioning in the presence of nitrite, based on prior reports that nitrite strongly inhibits the periplasmic [Fe] hydrogenase but has no impact on [NiFe] hydrogenase (2). Thus, the redundancy in periplasmic hydrogenases may allow for functional compensation under stress conditions (19).

Furthermore, the up-regulation of periplasmic formate dehydrogenase points to the possibility that formate oxidation acts as another mechanism to supply electrons and protons for nitrite reduction, but the source of formate in the periplasm needs to be resolved. Interestingly, it is proposed that the "hydrogen cycling" model (43) for contributing to a proton gradient could potentially be one example of a more general phenomenon termed redox cycling (22). In fact, consideration of the *D. vulgaris* genome sequence reveals the potential for production of formate in the cytoplasm. Movement of the protonated, uncharged species through the cytoplasmic membrane and its oxidation in the periplasm could contribute to the electron and proton flows across the membrane (19). Thus, it is possible that uncharged formate generated during pyruvate oxidation diffuses across the membrane and then is oxidized by the formate dehydrogenase to contribute to the electrons and protons used in nitrite reduction or hydrogen generation.

The transcriptional response to nitrite stress in energy metabolism pathways also appeared to affect the expression of genes involved in nitrogen metabolism in *D. vulgaris* (Table 2). The down-regulation of multiple genes encoding ATP-requiring ABC amino acid and polyamine transporters may reflect the inhibition of ATP generation from sulfate respiration and/or the decreased demand for amino acids for protein biosynthesis. In contrast, the up-regulation of the glutamine synthetase gene (*glnA*) would appear to signal nitrogen-limiting conditions (31, 64). It is possible that an increased flux of carbon to support substrate level phosphorylation might overflow into the tricarboxylic acid cycle, altering the α-ketoglutarate/glutamine ratio controlling *glnA* expression. Another strategy to preserve amino acids for biosynthetic demand was the repression of genes encoding aspartate ammonia-lyase and asparaginase, which catabolize amino acids when they are present in excess.

Interestingly, results from this study show that genes in the Fur regulon were among the most highly up-regulated genes in response to nitrite stress (Table 3). As Fur is known as the primary regulator of iron homeostasis in many other microorganisms (30, 34), this observation raises a question about the connection between nitrite stress and iron homeostasis. The Fur family metalloregulatory proteins are typically dimeric DNA-binding transcriptional factors that also bind Fe^{2+} as a corepressor in order to repress downstream genes. It is therefore proposed that derepression of Fur-regulated genes could be attributed to interactions of nitrite, directly or indirectly, with either the Fur protein, Fe^{2+}, or both. Derepression of the Fur regulon could be effected by iron deficiency resulting from consumption of cytoplasmic Fe(II), since genes encoding many iron-containing proteins, including the nitrite reductase, were up-regulated in response to nitrite. Compounding this demand for iron, chemical oxidation of Fe^{2+} by NO_2^- has been readily observed (6, 42), and Fe^{3+} is generally unavailable for biosynthesis or signaling. A less likely mechanism is that nitrite might react directly with the protein-bound Fe^{2+} corepressor, generating Fe^{3+}, leading to dissociation and concomitant derepression. The intracellular concentrations of NO_2^- are likely to be small because of the rapid reduction of nitrite in the periplasm and the apparent absence of a specific transport system for this ion. However, given the complex chemistry of reactive nitrogen species (46), it is still possible that reactive nitrogen species generated from nitrite reduction could enter the cytoplasm to react with Fe^{2+} (8). However, the contribution of each mechanism to the relief from Fur repression during nitrite exposure is not clear, and further biochemical study is needed to address the mechanism and importance of Fur regulation in this stress response in *D. vulgaris*.

Since both Fur and PerR respond to oxidative stress and belong to the same superfamily of metalloregulatory proteins that respond to metal ions (33), it is possible that the same mechanism derepresses both regulons. Studies on other microorganisms have shown that reactive nitrogen species, including nitrite, incidentally induce genes responsive to oxidative stress, in addition to genes specifically designed to protect cells from nitrosative stress (35, 36). Whether proteins encoded in the PerR regulon confer protection against nitrite or are adventitiously derepressed remains to be determined.

In summary, the results reveal that *D. vulgaris* cells initiate a coordination of transcriptional regulations allowing the alleviation of nitrite toxicity via nitrite reduction. The down-regulation of genes in the energy metabolism pathways suggests a shift in the flow of reducing equivalents from oxidative phosphorylation to nitrite reduction. Based on the transcriptional response to nitrite stress, it is also proposed that substrate level phosphorylation becomes prominent and that the excess reductant generated may be disposed of as succinate or hydrogen. It is further suggested that increased demand for iron resulting from these regulatory events likely contributes to iron depletion along with the chemical oxidation of available Fe^{2+}, derepressing the Fur regulon. However, further biochemical study is needed to elucidate the regulatory mechanisms and

importance of transcriptional regulators in *D. vulgaris* during stress responses.

ACKNOWLEDGMENTS

This research was supported by the U.S. Department of Energy under the Genomics: GTL Program through the Virtual Institute for Microbial Stress and Survival and Microbial Genome Program of the Office of Biological and Environmental Research, Office of Science. Oak Ridge National Laboratory is managed by University of Tennessee-Battelle LLC for the Department of Energy under contract DEAC05-00OR22725.

REFERENCES

1. **Altschul, S., T. Madden, A. Schäffer, J. Zhang, W. Miller, and D. Lipman.** 1997. Gapped BLAST and PSI-BLAST: a new generation of protein database search programs. Nucleic Acids Res. **25:**3389–3402.
2. **Berlier, Y., G. D. Fauque, J. LeGall, E. S. Choi, H. D. Peck, Jr., and P. A. Lespinat.** 1987. Inhibition studies of three classes of *Desulfovibrio* hydrogenase: application to the further characterization of the multiple hydrogenases found in *Desulfovibrio vulgaris* Hildenborough. Biochem. Biophys. Res. Commun. **146:**147–153.
3. **Betlach, M. R., and J. M. Tiedje.** 1981. Kinetic explanation for accumulation of nitrite, nitric oxide, and nitrous oxide during bacterial denitrification. Appl. Environ. Microbiol. **42:**1074–1084.
4. **Bozdech, Z., J. C. Zhu, M. P. Joachimiak, F. E. Cohen, B. Pulliam, and J. L. DeRisi.** 2003. Expression profiling of the schizont and trophozoite stages of *Plasmodium falciparum* with a long-oligonucleotide microarray. Genome Biol. **4:**R9. [Online.] doi:10.1186/gb-2003-4-2-r9.
5. **Brandis, A., and R. K. Thauer.** 1981. Growth of *Desulfovibrio* species on hydrogen and sulfate as sole energy source. J. Gen. Microbiol. **126:**249–252.
6. **Brons, H. J., W. R. Hagen, and A. J. Zehnder.** 1991. Ferrous iron dependent nitric oxide production in nitrate reducing cultures of *Escherichia coli*. Arch. Microbiol. **155:**341–347.
7. **Chardin, B., A. Dolla, F. Chaspoul, M. L. Fardeau, P. Gallice, and M. Bruschi.** 2002. Bioremediation of chromate: thermodynamic analysis of the effects of Cr(VI) on sulfate-reducing bacteria. Appl. Microbiol. Biotechnol. **60:**352–360.
8. **D'Autréaux, B., D. Touati, B. Bersch, J.-M. Latour, and I. Michaud-Soret.** 2002. Direct inhibition by nitric oxide of the transcriptional ferric uptake regulation protein via nitrosylation of the iron. Proc. Natl. Acad. Sci. USA **99:**16619–16624.
9. **Davidova, I., M. S. Hicks, P. M. Fedorak, and J. M. Suflita.** 2001. The influence of nitrate on microbial processes in oil industry production waters. J. Ind. Microbiol. Biotechnol. **27:**80–86.
10. **Escolar, L., J. Perez-Martin, and V. de Lorenzo.** 1999. Opening the iron box: transcriptional metalloregulation by the Fur protein. J. Bacteriol. **181:**6223–6229.
11. **Gadd, G. M., and C. White.** 1993. Microbial treatment of metal pollution—a working biotechnology? Trends Biotechnol. **11:**353–359.
12. **Gao, H., Y. Wang, X. Liu, T. Yan, L. Wu, E. Alm, A. Arkin, D. K. Thompson, and J. Zhou.** 2004. Global transcriptome analysis of the heat shock response of *Shewanella oneidensis*. J. Bacteriol. **186:**7796–7803.
13. **Greene, E. A., C. Hubert, M. Nemati, G. E. Jenneman, and G. Voordouw.** 2003. Nitrite reductase activity of sulphate-reducing bacteria prevents their inhibition by nitrate-reducing, sulphide-oxidizing bacteria. Environ. Microbiol. **5:**607–617.
14. **Hantke, K.** 2001. Iron and metal regulation in bacteria. Curr. Opin. Microbiol. **4:**172–177.
15. **Hao, O. J., J. M. Chen, L. Huang, and R. L. Buglass.** 1996. Sulfate-reducing bacteria. Crit. Rev. Environ. Sci. Technol. **26:**155–187.
16. **Haveman, S. A., E. A. Greene, C. P. Stilwell, J. K. Voordouw, and G. Voordouw.** 2004. Physiological and gene expression analysis of inhibition of *Desulfovibrio vulgaris* Hildenborough by nitrite. J. Bacteriol. **186:**7944–7950.
17. **He, Q., and K. R. Mankin.** 2002. Assessing removal kinetics of organic matter in rock-plant filters. Trans. Am. Soc. Agric. Eng. **45:**1771–1778.
18. **He, Z., L. Wu, X. Li, M. W. Fields, and J. Zhou.** 2005. Empirical establishment of oligonucleotide probe design criteria. Appl. Environ. Microbiol. **71:**3753–3760.
19. **Heidelberg, J. F., R. Seshadri, S. A. Haveman, C. L. Hemme, I. T. Paulsen, J. F. Kolonay, J. A. Eisen, N. Ward, B. Methe, L. M. Brinkac, S. C. Daugherty, R. T. Deboy, R. J. Dodson, A. S. Durkin, R. Madupu, W. C. Nelson, S. A. Sullivan, D. Fouts, D. H. Haft, J. Selengut, J. D. Peterson, T. M. Davidsen, N. Zafar, L. Zhou, D. Radune, G. Dimitrov, M. Hance, K. Tran, H. Khouri, J. Gill, T. R. Utterback, T. V. Feldblyum, J. D. Wall, G. Voordouw, and C. M. Fraser.** 2004. The genome sequence of the anaerobic, sulfate-reducing bacterium *Desulfovibrio vulgaris* Hildenborough. Nat. Biotechnol. **22:**554–559.
20. **Hubert, C., M. Nemati, G. E. Jenneman, and G. Voordouw.** 2005. Corrosion risk associated with microbial souring control using nitrate or nitrite. Appl. Microbiol. Biotechnol. **68:**272–282.
21. **Jenneman, G. E., M. J. McInerney, and R. M. Knapp.** 1986. Effect of nitrate on biogenic sulfide production. Appl. Environ. Microbiol. **51:**1205–1211.
22. **Jormakka, M., B. Byrne, and S. Iwata.** 2003. Proton motive force generation by a redox loop mechanism. FEBS Lett. **545:**25–30.
23. **Kelso, B. H. L., R. V. Smith, and R. J. Laughlin.** 1999. Effects of carbon substrates on nitrite accumulation in freshwater sediments. Appl. Environ. Microbiol. **65:**61–66.
24. **Little, B. J., R. I. Ray, and R. K. Pope.** 2000. Relationship between corrosion and the biological sulfur cycle: a review. Corrosion **56:**433–443.
25. **Lloyd, J. R., J. Ridley, T. Khizniak, N. N. Lyalikova, and L. E. Macaskie.** 1999. Reduction of technetium by *Desulfovibrio desulfuricans*: biocatalyst characterization and use in a flowthrough bioreactor. Appl. Environ. Microbiol. **65:**2691–2696.
26. **Londry, K. L., and J. M. Suflita.** 1999. Use of nitrate to control sulfide generation by sulfate-reducing bacteria associated with oily waste. J. Ind. Microbiol. Biotechnol. **22:**582–589.
27. **Lovley, D. R., E. E. Roden, E. J. P. Phillips, and J. C. Woodward.** 1993. Enzymatic iron and uranium reduction by sulfate-reducing bacteria. Marine Geol. **113:**41–53.
28. **Lovley, D. R., P. K. Widman, J. C. Woodward, and E. J. P. Phillips.** 1993. Reduction of uranium by cytochrome c_3 of *Desulfovibrio vulgaris*. Appl. Environ. Microbiol. **59:**3572–3576.
29. **Madigan, M. T., J. M. Martinko, and J. Parker.** 2000. Brock biology of microorganisms. Prentice-Hall, Upper Saddle River, N.J.
30. **McHugh, J. P., F. Rodríguez-Quiñones, H. Abdul-Tehrani, D. A. Svistunenko, R. K. Poole, C. E. Cooper, and S. C. Andrews.** 2003. Global iron-dependent gene regulation in *Escherichia coli*: a new mechanism for iron homeostasis. J. Biol. Chem. **278:**29478–29486.
31. **Merrick, M. J., and R. A. Edwards.** 1995. Nitrogen control in bacteria. Microbiol. Rev. **59:**604–622.
32. **Mitchell, G. J., J. G. Jones, and J. A. Cole.** 1986. Distribution and regulation of nitrate and nitrite reduction by *Desulfovibrio* and *Desulfotomaculum* species. Arch. Microbiol. **144:**35–40.
33. **Mongkolsuk, S., and J. D. Helmann.** 2002. Regulation of inducible peroxide stress responses. Mol. Microbiol. **45:**9–15.
34. **Moore, C. M., and J. D. Helmann.** 2005. Metal ion homeostasis in *Bacillus subtilis*. Curr. Opin. Microbiol. **8:**188–195.
35. **Moore, C. M., M. M. Nakano, T. Wang, R. W. Ye, and J. D. Helmann.** 2004. Response of *Bacillus subtilis* to nitric oxide and the nitrosating agent sodium nitroprusside. J. Bacteriol. **186:**4655–4664.
36. **Mukhopadhyay, P., M. Zheng, L. A. Bedzyk, R. A. LaRossa, and G. Storz.** 2004. Prominent roles of the NorR and Fur regulators in the *Escherichia coli* transcriptional response to reactive nitrogen species. Proc. Natl. Acad. Sci. USA **101:**745–750.
37. **Mulder, N. J., R. Apweiler, T. K. Attwood, A. Bairoch, A. Bateman, D. Binns, P. Bradley, P. Bork, P. Bucher, L. Cerutti, R. Copley, E. Courcelle, U. Das, R. Durbin, W. Fleischmann, J. Gough, D. Haft, N. Harte, N. Hulo, D. Kahn, A. Kanapin, M. Krestyaninova, D. Lonsdale, R. Lopez, I. Letunic, M. Madera, J. Maslen, J. McDowall, A. Mitchell, A. N. Nikolskaya, S. Orchard, M. Pagni, C. P. Ponting, E. Quevillon, J. Selengut, C. J. Sigrist, V. Silventoinen, D. J. Studholme, R. Vaughan, and C. H. Wu.** 2005. InterPro, progress and status in 2005. Nucleic Acids Res. **33:**D201–D205.
38. **Myhr, S., B. L. P. Lillebo, E. Sunde, J. Beeder, and T. Torsvik.** 2002. Inhibition of microbial H_2S production in an oil reservoir model column by nitrate injection. Appl. Microbiol. Biotechnol. **58:**400–408.
39. **Natural and Accelerated Bioremediation Research Program.** 2003. Bioremediation of metals and radionuclides: what it is and how it works, p. 1–78. *In* T. C. Hazen, S. M. Benson, F. B. Metting, B. Faison, A. C. Palmisano, and J. McCullough (ed.), NABIR primer, 2nd ed. Lawrence Berkeley National Laboratory, Berkeley, Calif.
40. **Nemati, M., T. J. Mazutinec, G. E. Jenneman, and G. Voordouw.** 2001. Control of biogenic H_2S production with nitrite and molybdate. J. Ind. Microbiol. Biotechnol. **26:**350–355.
41. **Nunoshiba, T., T. DeRojas-Walker, J. S. Wishnok, S. R. Tannenbaum, and B. Demple.** 1993. Activation by nitric oxide of an oxidative-stress response that defends *Escherichia coli* against activated macrophages. Proc. Natl. Acad. Sci. USA **90:**9993–9997.
42. **Obuekwe, C. O., D. W. Westlake, and F. D. Cook.** 1981. Effect of nitrate on reduction of ferric iron by a bacterium isolated from crude oil. Can. J. Microbiol. **27:**692–697.
43. **Odom, J. M., and H. D. Peck, Jr.** 1981. Hydrogen cycling as a general mechanism for energy coupling in the sulfate-reducing bacteria, *Desulfovibrio* sp. FEMS Microbiol. Lett. **12:**47–50.
44. **Pereira, I. A. C., J. LeGall, A. V. Xavier, and M. Teixeira.** 2000. Characterization of a heme *c nitrite reductase from a non-ammonifying microorganism*, *Desulfovibrio vulgaris* Hildenborough. Biochim. Biophys. Acta **1481:**119–130.
45. **Peterson, J. D., L. A. Umayam, T. Dickinson, E. K. Hickey, and O. White.** 2001. The comprehensive microbial resource. Nucleic Acids Res. **29:**123–125.
46. **Poole, R. K.** 2005. Nitric oxide and nitrosative stress tolerance in bacteria. Biochem. Soc. Trans. **33:**176–180.

47. **Postgate, J. R.** 1984. The sulfate-reducing bacteria, 2nd ed. Cambridge University Press, Cambridge, United Kingdom.
48. **Price, M. N., K. H. Huang, E. J. Alm, and A. P. Arkin.** 2005. A novel method for accurate operon predictions in all sequenced prokaryotes. Nucleic Acids Res. **33:**880–892.
49. **Riley, R. G., and J. Zachara.** 1992. Chemical contaminants on DOE lands and selection of contaminant mixtures for subsurface research, DOE/ER-0547T. U.S. Department of Energy, Washington, D.C.
50. **Rodionov, D. A., I. Dubchak, A. P. Arkin, E. Alm, and M. S. Gelfand.** 2004. Reconstruction of regulatory and metabolic pathways in metal-reducing δ-proteobacteria. Genome Biol. **5:**R90. [Online.] doi:10.1186/gb-2004-5-11-r90.
51. **Rouillard, J. M., C. J. Herbert, and M. Zuker.** 2002. OligoArray: genome-scale oligonucleotide design for microarrays. Bioinformatics **18:**486–487.
52. **Rozen, S., and H. J. Skaletsky.** 2000. Primer3 on the WWW for general users and for biologist programmers, p. 365–386. *In* S. Krawetz and S. Misener (ed.), Bioinformatics methods and protocols: methods in molecular biology. Humana Press, Totowa, N.J.
53. **Seo, J., M. Bakay, Y.-W. Chen, S. Hilmer, B. Shneiderman, and E. P. Hoffman.** 2004. Interactively optimizing signal-to-noise ratios in expression profiling: project-specific algorithm selection and detection *p*-value weighting in Affymetrix microarrays. Bioinformatics **20:**2534–2544.
54. **Singleton, R., Jr.** 1993. The sulfate-reducing bacteria: an overview, p. 1–21. *In* J. M. Odom and R. Singleton, Jr. (ed.), The sulfate-reducing bacteria: contemporary perspectives. Springer-Verlag, New York, N.Y.
55. **Thompson, D. K., A. S. Beliaev, C. S. Giometti, S. L. Tollaksen, T. Khare, D. P. Lies, K. H. Nealson, H. Lim, J. Yates, C. C. Brandt, J. M. Tiedje, and J. Zhou.** 2002. Transcriptional and proteomic analysis of a ferric uptake regulator (Fur) mutant of *Shewanella oneidensis*: possible involvement of Fur in energy metabolism, transcriptional regulation, and oxidative stress. Appl. Environ. Microbiol. **68:**881–892.
56. **Valls, M., and V. de Lorenzo.** 2002. Exploiting the genetic and biochemical capacities of bacteria for the remediation of heavy metal pollution. FEMS Microbiol. Rev. **26:**327–338.
57. **van den Berg, W. A. M., W. R. Hagen, and W. M. A. M. van Dongen.** 2000. The hybrid-cluster protein ("prismane protein") from *Escherichia coli*: characterization of the hybrid-cluster protein, redox properties of the [2Fe-2S] and [4Fe-2S–2O] clusters and identification of an associated NADH oxidoreductase containing FAD and [2Fe-2S]. Eur. J. Biochem. **267:**666–676.
58. **van Rijn, J., Y. Tal, and Y. Barak.** 1996. Influence of volatile fatty acids on nitrite accumulation by a *Pseudomonas stutzeri* strain isolated from a denitrifying fluidized bed reactor. Appl. Environ. Microbiol. **62:**2615–2620.
59. **Wan, X.-F., N. C. VerBerkmoes, L. A. McCue, D. Stanek, H. Connelly, L. J. Hauser, L. Wu, X. Liu, T. Yan, A. Leaphart, R. L. Hettich, J. Zhou, and D. K. Thompson.** 2004. Transcriptomic and proteomic characterization of the Fur modulon in the metal-reducing bacterium *Shewanella oneidensis*. J. Bacteriol. **186:**8385–8400.
60. **Wang, X. W., and B. Seed.** 2003. Selection of oligonucleotide probes for protein coding sequences. Bioinformatics **19:**796–802.
61. **White, C., J. A. Sayer, and G. M. Gadd.** 1997. Microbial solubilization and immobilization of toxic metals: key biogeochemical processes for treatment of contamination. FEMS Microbiol. Rev. **20:**503–516.
62. **Wolfe, B. M., S. M. Lui, and J. A. Cowan.** 1994. Desulfoviridin, a multimeric-dissimilatory sulfite reductase from *Desulfovibrio vulgaris* (Hildenborough): purification, characterization, kinetics and EPR studies. Eur. J. Biochem. **223:**79–89.
63. **Wolfe, M. T., J. Heo, J. S. Garavelli, and P. W. Ludden.** 2002. Hydroxylamine reductase activity of the hybrid cluster protein from *Escherichia coli*. J. Bacteriol. **184:**5898–5902.
64. **Woods, D. R., and S. J. Reid.** 1993. Recent developments on the regulation and structure of glutamine synthetase enzymes from selected bacterial groups. FEMS Microbiol. Rev. **11:**273–284.